Route to chaos for a global variable of a two-dimensional 'game-of-life type' automata network

1994 J. Phys. A: Math. Gen. 27 8039

(http://iopscience.iop.org/0305-4470/27/24/015)

J. Phys. A: Math. Gen. 27 (1994) 8039–8047. Printed in the UK

Route to chaos for a global variable of a two-dimensional 'game-of-life type' automata network

Nino Boccara†‡, Olivier Roblin†§ and Michel Roger†

† DRECAM-SPEC, CE Saclay, 91191 Gif-sur-Yvette Cedex, France
‡ Department of Physics, University of Illinois, Chicago, IL 60607-7059, USA
§ Ecole Supérieure d'Electricité, 91192 Gif-sur-Yvette Cedex, France

Received 27 June 1994, in final form 18 October 1994

Abstract. We consider a two-dimensional cellular automaton whose rule consists of two subrules. The first, applied synchronously, is a local rule inspired from the 'game of life', with a larger neighbourhood. The second, applied sequentially, describes the motion of a fraction m of individuals. Such rules appear to be useful for modelling complex systems in ecology, such as natural populations of animals, in which the motion of the individuals is believed to play an important role. If the motion is long-range, the density of individuals exhibits a sequence of period-doubling bifurcations and behaves chaotically when m is large enough. If the motion is short-range (i.e. restricted to first neighbours), patterns become inhomogeneous. Spatial correlations decay with a finite correlation length ξ of the order of $\sqrt{m}$. We observe the formation of domains, of mean width ξ, with a chaotic behaviour of the local density of individuals, but the collective behaviour is stationary (the global density tends to a fixed value when the lattice size is much larger than $\xi \times \xi$).

1. Introduction

Natural populations of plants and animals exhibit various patterns of fluctuations about long-term averages. Many species have a roughly constant population density while others exhibit large fluctuations with cyclic or quasi-cyclic behaviour. An excellent introduction to this topic is given by May (1985). A well known example is the fluctuations of the Canadian lynx population as documented in the data compiled by the Hudson Bay Company over the period 1735–1940. Oscillations with a roughly constant period of about 10 years are observed with large amplitude fluctuations, which, as stressed by Schaffer (1984, 1985), could correspond to chaotic behaviour.

May has shown how simple deterministic models based on finite-difference equations can lead to complex behaviour. The dynamics of a single population density c is usually modelled by a simple finite-difference equation

$$c(t+1) = F[c(t)] \tag{1}$$

which means that birth and death rates depend only on the global population density $c(t)$. The relation is likely to be such that relatively low values of c increase rapidly from one generation to the next while relatively high values of c tend to decrease. Hence the nonlinear function F has a characteristic shape with a maximum, which can lead, as a function of its curvature, to chaos through the familiar cascade of period-doubling bifurcations (Feigenbaum 1978).

0305-4470/94/248039+09$19.50

Unfortunately, such a global description does not take into account the local character of individual behaviour. Cellular automata networks offer a simple and natural frame for a more subtle model including the local interaction between individuals.

A single population on a discrete two-dimensional lattice is represented by a two-dimensional automata network. Each site is either vacant (state 0) or occupied by one individual (state 1). A realistic model for the time evolution of *animal populations* should include both local interactions and possible motion of individuals. Hence we consider an automaton rule which consists of two subrules.

(i) The first one, applied synchronously, is a standard deterministic cellular automaton rule, which models local interactions between the individuals. Following the global models for population dynamics discussed by May, here we assume that the *local* birth or death rate at site i only depends on the *local* population density (i.e. total number of 1 in a finite neighbourhood). More precisely we choose an *outer totalistic law* defined on a *Moore-type neighbourhood*—cf Wolfram (1983)—i.e. the state $s(t+1, i)$ of the site i at time $t+1$ is a function $f(s(t, i), \sigma(t, i))$ of the state $s(t, i)$ at time t and of the sum

$$\sigma(t, i) = \sum_{j \in \mathcal{M}(i)} s(t, j) .$$

The Moore-type neighbourhood $\mathcal{M}(i)$ of site i contains all sites deduced from i by a translation $\tau = px + qy$, where p and q are non-zero integers varying between $-r$ and r (r is the range of the rule). x and y are elementary translation vectors on a square lattice:

$$f(1, \sigma) = \begin{cases} 1 & \text{if} \quad S_{\min} \leqslant \sigma \leqslant S_{\max} \\ 0 & \text{otherwise} \end{cases}$$

$$f(0, \sigma) = \begin{cases} 1 & \text{if} \quad B_{\min} \leqslant \sigma \leqslant B_{\max} \\ 0 & \text{otherwise} . \end{cases}$$

Such rules are inspired by the 'game of life', i.e. individuals survive if the neighbourhood is not too crowded or too poorly populated and birth also occurs at a vacant site if the number of neighbours satisfies some stringent constraints. We expect such rules to apply quite generally to animals which cannot survive if they are isolated and which die from food scarcity if the neighbourhood is too crowded.

(ii) The second one, which describes the motion of the individuals, moves sequentially over a fraction of non-zero sites. More precisely, an individual (non-zero site) selected at random is moved to a site, also selected at random, if this site is empty (zero site). The motion can be long-range (a non-zero site can move to any site) or short-range (i.e. restricted to first neighbours). This operation is repeated $m \times c(m, t) \times N$ times, where N is the total number of sites, and $c(m, t)$ the density of non-zero sites at time t. It is important to note that, although this process does not change the number of individuals, it partially destroys the correlations created by the basic automaton without mixing. Starting from the same initial condition, the time evolution of the concentration will be different from that obtained with the basic automaton without mixing and c depends both on m and t. With this definition, the number of effective moves of non-zero sites is $mc(m, t)(1 - c(m, t))N$.

When m is large, all the correlations created by the cellular-automaton rule are destroyed, and the evolution of the density of non-zero sites is correctly predicted by a mean-field-type

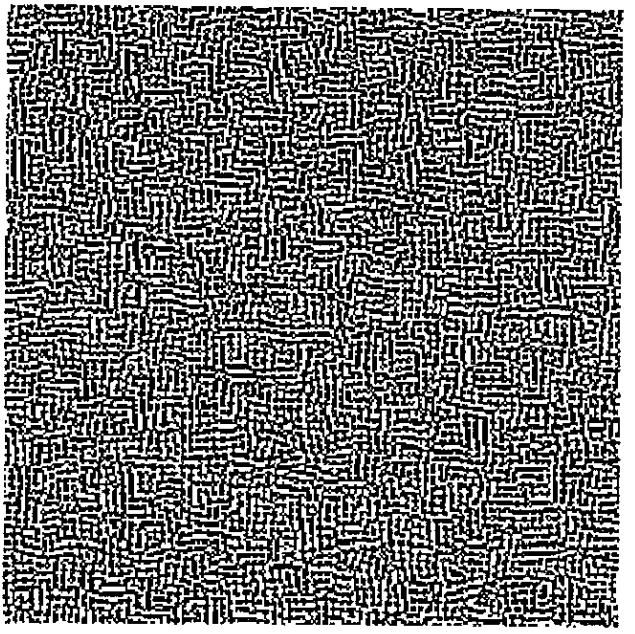

Figure 1. Stationary state obtained with $m = 0$, after a few hundred time steps, starting from a random distribution of non-zero sites with $c(0, 0) = 0.5$ on a 256×256 lattice.

approximation, which otherwise is often far from being correct in the absence of motion (Bidaux *et al* 1989, Chaté and Manneville 1991). The population dynamics obeys an equation similar to (1).

As a typical and realistic example for a single population we choose

$$r = 2 \qquad S_{\min} = 7 \qquad S_{\max} = 14 \qquad B_{\min} = 8 \qquad B_{\max} = 10.$$

For $m = 0$, starting from a random distribution of $c(0, 0) = 0.5$ non-zero sites, we obtain a stable configuration after a few hundred time steps, as shown in figure 1. This rule is of class 2, according to Wolfram's classification (1983). For sufficiently large m, the population dynamics are correctly predicted by a mean-field approximation. The mean-field approximation ignores space dependence and neglects correlations. The mean-field evolution for the density $c(t)$ of non-zero sites a time t reads

$$c(t+1) = c(t)\sum_{i=7}^{14}\binom{24}{i}c(t)^i\big(1-c(t)\big)^{24-i} + \big(1-c(t)\big)\sum_{i=8}^{10}\binom{24}{i}c(t)^i\big(1-c(t)\big)^{24-i}. \tag{2}$$

It has a chaotic temporal behaviour.

It is very interesting to study the behaviour of this automata network for intermediate values of the mixing parameter m.

A preliminary academic study on some one-dimensional class-3 cellular automaton rules with long-range moves has been published by Boccara and Roger (1992). The first part of the paper is a generalization to two-dimensional models which are more realistic for modelling ecological systems. The results are basically the same (they do not depend

on the dimension or on the class of the rule). For long-range moves, as m increases, the stationary value of the density of non-zero sites follows a route to chaos through the familiar cascade of period-doubling bifurcations.

In the second part we show that for short-range moves the behaviour is rather different. As m increases, the patterns become inhomogeneous. Spatial correlations decay with a finite correlation length ξ of the order of $\sqrt{m}$. We observe the formation of domains of mean width of the order of ξ with a chaotic local density. However, when the size of the lattice is much larger than $\xi \times \xi$, the global density of non-zero sites tends to a fixed point.

A similar behaviour with spatial disorder and stationary collective variables is generally obtained in one-dimensional lattices of coupled logistic maps with periodic boundary conditions (Kaneko 1984, Bohr *et al* 1987, Rasmussen and Bohr 1987), while more striking non-trivial collective behaviours are observed in higher dimensions (Chaté and Manneville 1992).

2. Long-range moves

For long-range moves, the results are similar to those obtained in one-dimension with class-3 rules (Boccara and Roger 1992). For small m, the density of non-zero sites $c(m, t)$ tends to a fixed point $c(m, \infty)$ as t tends to ∞. As m increases, the stationary value of the density of non-zero sites follows a route to chaos through the familiar cascade of period-doubling bifurcations. The bifurcation diagram for a 1024×1024 lattice is shown in figure 2. m is varied adiabatically by steps of 0.025 (figure 2(a)) or 0.005 (figure 2(b)), i.e. after varying m we start from the configuration obtained at large time for the preceding m. For each value of m, the first 100 iterations are discarded and the values of the density $c(m, t)$ for the next 100 iterations are plotted on the diagram of figure 2(a). Figure 2(b) represents an enlargement of the bifurcation diagram close to the second and third bifurcations. To improve the observation of the period-8 cycle, points are averaged over 12 cycles.

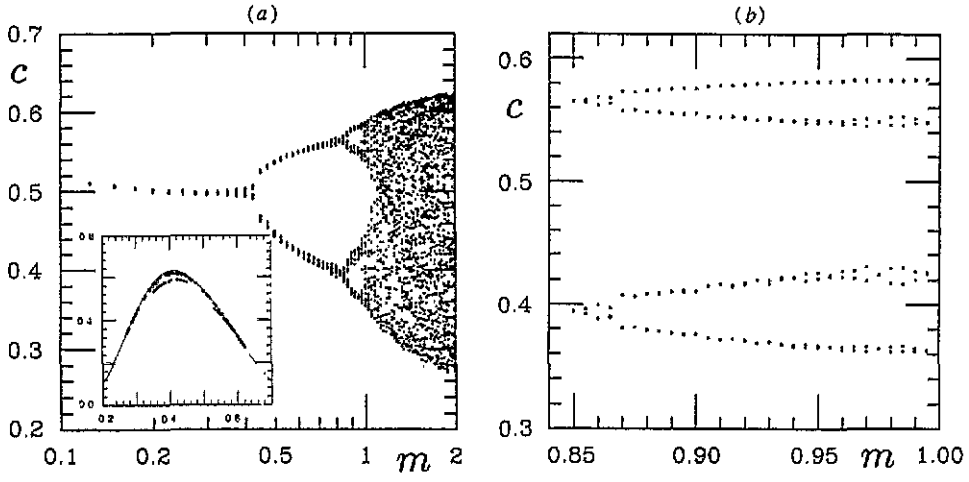

Figure 2. Bifurcation diagram for the stationary value $c(m, \infty)$ of the density of non-zero sites for long-range moves. (a) Overall diagram with $N = 1024 \times 1024$ sites. (b) An enlargement of the region corresponding to the second and third bifurcation. To improve the observation of the period-8 cycle the points shown here represent averages over 12 cycles. For different values of t the inset shows a plot of $c(m, t+1)$ versus $c(m, t)$ with $m = 1$ (+) and $m = 2$ (o). As m increases, the points come close to the mean-field map (full curve) represented by (2).

The first three bifurcation points are $m_1 = 0.420 \pm 0.005$, $m_2 = 0.865 \pm 0.005$ and $m_3 = 0.955 \pm 0.005$. Due to the fact that the size of the lattice is finite, the full sequence of period-doubling bifurcations cannot be observed. The Feigenbaum constant δ (Feigenbaum 1978) is the limit as n goes to ∞ of the sequence (δ_n), where $\delta_n = (m_{n+1} - m_n)/(m_{n+2} - m_{n+1})$. From the first three bifurcation points, we find that $\delta_1 = 4.9 \pm 0.5$, which is compatible with the universal value 4.67 obtained for δ_∞.

As shown in the inset of figure 2(*a*), when m is large, the dynamics are close to that predicted by the mean-field map (2).

3. Short-range moves

Figure 3 represents a diagram obtained for short-range moves on a 256×256 lattice, with the procedure used for figure 2(*a*). Although some chaotic behaviour appears on finite-size lattices for sufficiently large m, there is no evidence of a cascade of period-doubling bifurcations. Indeed, as m increases, patterns become inhomogeneous. Figure 4 compares, at two consecutive times, the patterns obtained with $m = 100$ on a 512×512 lattice. Figure 5 represents two patterns obtained at consecutive times with $m = 1600$ on the same lattice. We observe the formation of domains with regions of low and high densities of non-zero sites. Within a domain, the local density of non-zero sites oscillates. There are some similarities with the 'kink–anti-kink patterns' observed by Kaneko (1984) in a one-dimensional lattice of coupled logistic maps. However, here the frontiers between domains are highly mobile and it is difficult to follow one domain over more than 5–10 time steps. With m fixed, if the lattice size increases and becomes much larger than the mean size of domains, the global density of non-zero sites tends to a stationary value.

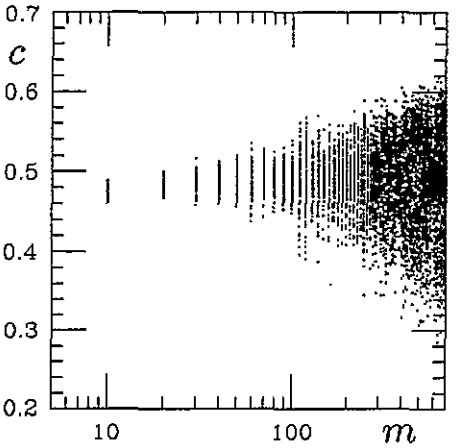

Figure 3. Same diagram as figure 2(*a*), with short-range moves on a 256×256 lattice.

The size of these domains increases with m. It is interesting to estimate it more quantitatively. The mean *width* of these domains has been computed as follows. After a transient of a few hundred time steps, we measure the mean density c of non-zero sites over about one hundred time steps. For a given pattern at time t, we define a local density $\bar{c}(x, y)$ as the mean concentration of non-zero sites in a 16×16 square centred at (x, y). We associate with each site at (x, y) a Boolean variable $b(x, y)$ which is *one* if $\bar{c}(x, y) > c$ and *zero* otherwise. Then on a given line y_0 we count the number of segments $\nu(l)$ corresponding

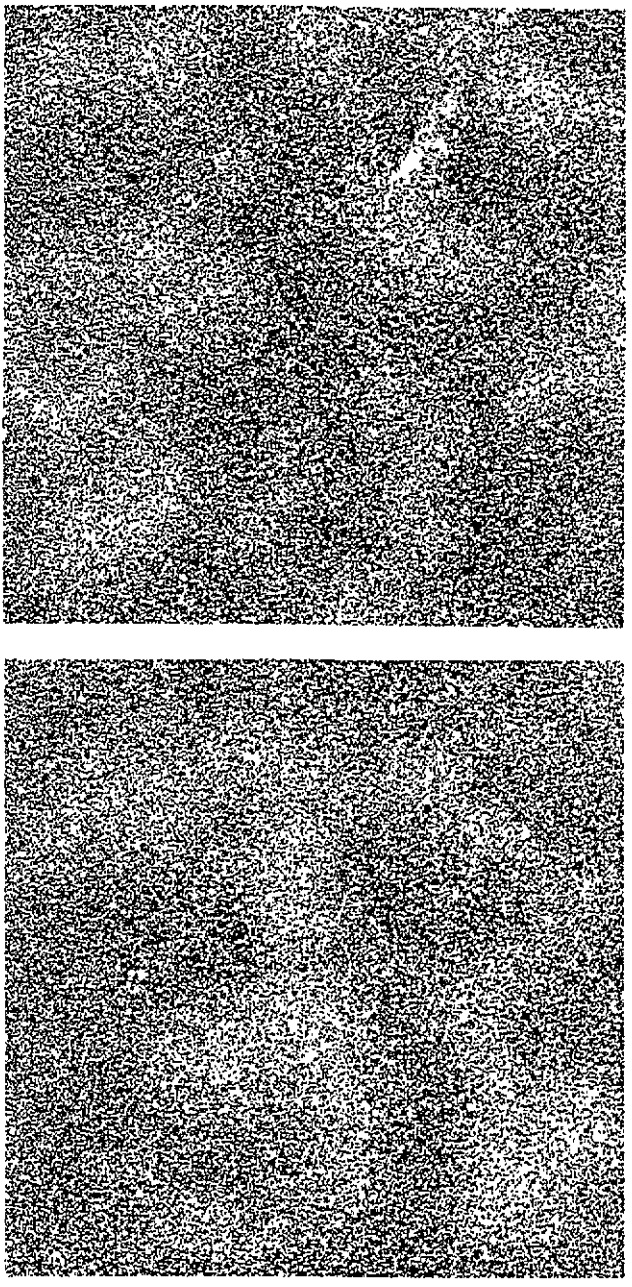

Figure 4. Typical patterns obtained at two consecutive times after about 100 time steps on a 512×512 lattice with $m = 200$.

to sequences of l *zeros* or l *ones* along x. We then sweep y and add the contributions of all lines. A mean value of $\nu(l)$ is obtained by averaging over 200 patterns obtained at consecutive time steps, after a transient of a few hundred time steps.

Figure 6 represents, on a semi-logarithmic scale, the results for $\nu(l)$ obtained with the same $m = 100$ and different lattice sizes. An interesting result is that the distribution $\nu(l)$

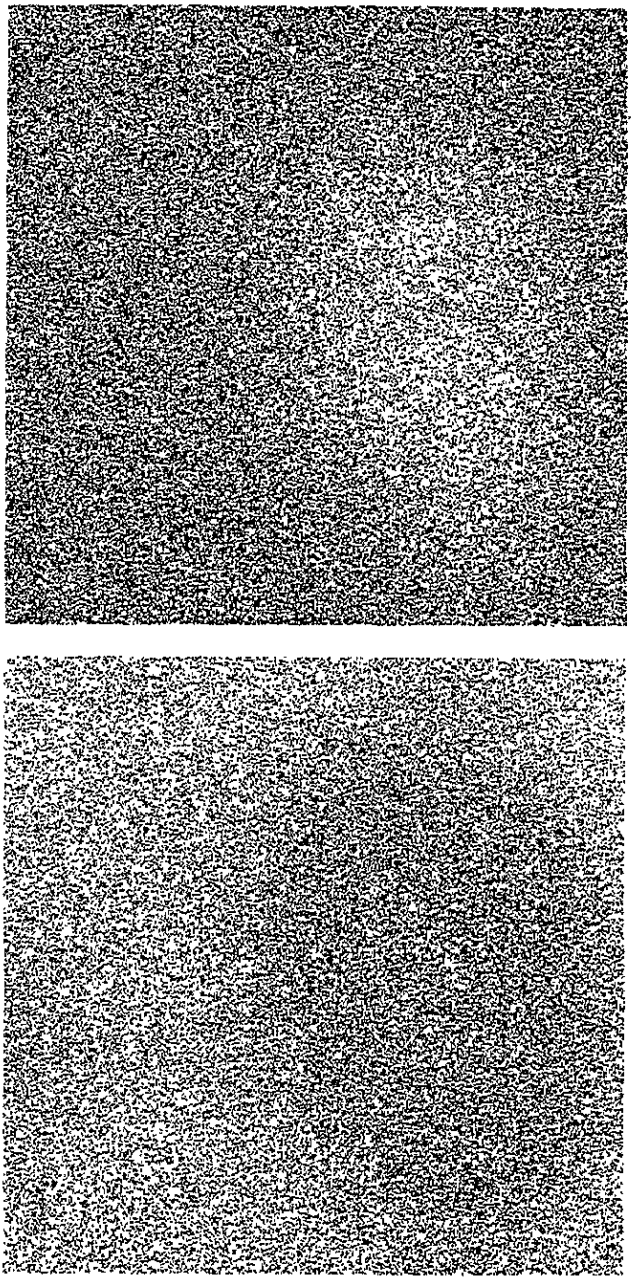

Figure 5. Same as figure 4, with $m = 1600$.

follows a simple exponential law. It is also clear from this figure that the domain *mean width* is independent of the lattice size N.

Figure 7 compares, for the same 512×512 lattice and different m, the distributions ν as a function of $l/\sqrt{m}$. The distributions of the *linear domain size* scale as $\nu(l) \approx \exp(-l/\zeta)$ with $\zeta = 4.1\sqrt{m}$. The characteristic length ζ gives an order of magnitude of the mean domain width, i.e. the mean area of the domains scales as m.

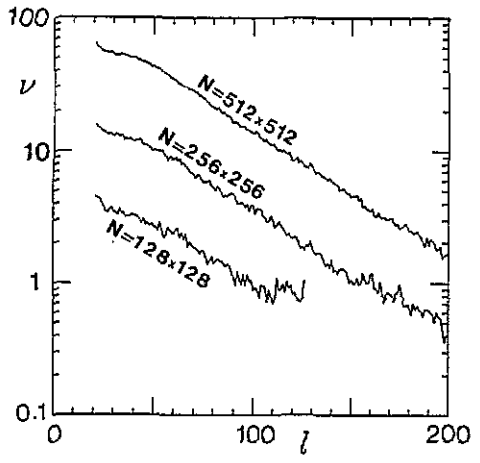

Figure 6. Domain-width distribution $\nu(l)$ as a function of l for various lattice sizes and same value of m ($m = 100$). As defined in the text, ν is proportional to the lattice area N.

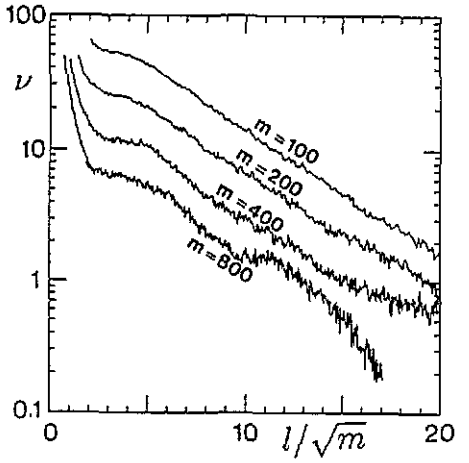

Figure 7. Domain-width distribution $\nu(\bar{l})$ as a function of $\bar{l} = l/\sqrt{m}$ for a 512 × 512 lattice and increasing values of m.

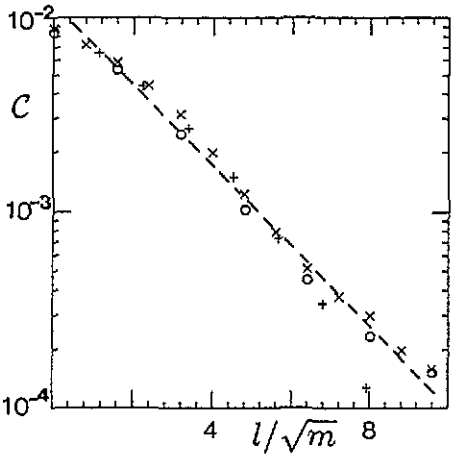

Figure 8. Semi-logarithmic plot of the spatial correlation function C in terms of $l/\sqrt{m}$: $m = 100$ (○), $m = 200$ (×) and $m = 400$ (+).

The loss of spatial coherence is generally characterized by a decay of the spatial correlations with a finite correlation length (see, for example, Rasmussen and Bohr 1987). On a 512 × 512 lattice we have measured the correlation function

$$C(l) = \langle (\bar{c}(i) - c)(\bar{c}(j) - c) \rangle \tag{3}$$

where c is the stationary value of the global concentration for $N \to \infty$ and $\bar{c}(i)$ is the 'local' concentration measured on a 16 × 16 square centred at i. The bracket represents the mean value over all pairs $\{i, j\}$ with distance $d(i, j) = l$ on the lattice. To improve the statistics, our values are averages over patterns obtained during a few hundred time steps after discarding a transient of about one hundred time steps. A semi-logarithmic plot of C as a function of $l/\sqrt{m}$ is represented in figure 8 for various m. The correlation function decays roughly exponentially with a correlation length of $\xi \approx 2.1\sqrt{m}$, of the same order of magnitude as ζ.

The short-range mixing corresponds to a diffusion process which moves non-zero sites over a distance $\sqrt{m}$ at each time step. The correlation length appears to be of the order of magnitude of the 'effective' range of the global rule defined for this model.

4. Conclusion

A specific ensemble of cellular automaton rules with local 'game-of-life type' interactions and short- or long-range motion of the individuals (non-zero sites) has been studied. Such rules are sufficiently realistic to model a variety of single-animal populations in ecology.

If the mean-field equation is chaotic, for long-range moves the stationary density of non-zero sites follows (as a function of the parameter m, characterizing the degree of mixing) a route to chaos through the usual period-doubling bifurcation cascade.

For short-range moves we do not observe a global chaotic behaviour, but spatial disorder characterized by an exponential decay of the correlation function with a finite correlation length ξ of the order of $\sqrt{m}$.

Patterns are split into domains of width of the order of ξ. In a domain, the local density of non-zero sites behaves chaotically. However, the mean density over the whole lattice tends to a fixed value as the lattice area increases much beyond $\xi \times \xi$ (i.e. much beyond m).

Such a model could have some relevance for quasi-periodic or chaotic behaviours observed in real single populations in ecology (May 1995, Schaffer 1984, 1985). Moreover the model exhibits, for short-range moves, an interesting behaviour with a chaotic time evolution at the scale of the mean displacements of individuals but a stationary value at larger scales which could be relevant for animals having a finite habitat.

As emphasized by May (1985), one should, however, keep in mind that isolated single populations are likely to be found only in laboratories. In the natural world, interactions with other species are usually very important. Coupled systems with two or more interacting populations are more realistic. More intricate predator–prey models (Boccara, Roblin, and Roger) or epidemic models (Boccara and Cheong 1992, 1993) with two interacting populations have been studied recently, using cellular automata. These models also exhibit complex dynamics with cyclic or quasi-cyclic behaviours.

References

Bidaux R, Boccara N and Chaté H 1989 *Phys. Rev.* A **39** 3094–105
Boccara N and Cheong K 1992 *J. Phys. A: Math. Gen.* **25** 2447–61
—— 1993 *J. Phys. A: Math. Gen.* **26** 3707–17
—— 1994 *J. Phys. A: Math. Gen.* **27** 1585–97
Boccara N, Roblin O and Roger M 1994 to be published
Boccara N and Roger M 1992 *J. Phys. A: Math. Gen.* **25** L1009–14
Bohr T, Grinstein G, He Y and Jayaprakash C 1987 *Phys. Rev. Lett.* **58** 2155–8
Chaté H and Manneville P 1991 *Europhys. Lett.* **14** 409–13
—— 1992 *Prog. Theor. Phys. (Japan)* **87** 1–60 and references therein
Feigenbaum M J 1978 *J. Stat. Phys.* **19** 25–52
Kaneko K 1984 *Prog. Theor. Phys. (Japan)* **72** 480–6
May R M 1985 *Proc. R. Soc.* B **228** 241–66 and references therein
Rasmussen D R and Bohr T 1987 *Phys. Lett.* **125A** 107–10
Schaffer W M 1984 *Am. Nat.* **124** 798–820
—— 1985 *Ecology* **66** 93–106
Wolfram S 1983 *Rev. Mod. Phys.* **55** 601–44